Supplemental Materials

Detailed Methods

Histology

Anesthetized animals were exsanguinated for serology, euthanized by perfusion through the left ventricle with saline until atrial effluents were clear, and the specimens were excised. The base of the host heart with aortic root, the host brachiocephalic artery, and the donor heart were post-fixed in 4% paraformaldehyde for 24 h at 4 °C, and embedded in paraffin. Alternatively, specimens were immediately frozen in OCT. Hematoxylin and eosin (H&E), elastin Van Gieson (EVG), von Kossa, and Alizarin red stains were performed on 5 μm-thick sections by a research core facility of Yale's Department of Pathology using standard techniques. Morphological analyses were performed in 3-5 sections by tracing the luminal, internal, and external elastic lamina perimeters to calculate intima and media areas using ImageJ software (National Institutes of Health, Bethesda, MD). For lipid detection, the aorta was dissected free of connective tissue and fat, excised, opened longitudinally, post-fixed in 4% paraformaldehyde, pinned onto a silicone plate luminal surface up, incubated with 0.2% Oil Red O solution (Sigma-Aldrich, St. Louis, MO) for 50 min at room temperature, destained in 78% methanol for 5 min, and then mounted on glass slides using aqueous mounting medium. Images were acquired using a Nikon SMZ 1000 microscope connected to a Kodak DC290 camera and multiple high power views were combined for each aorta. Lipid lesions were individually traced and the sum of their area to that of the whole aorta was quantified using ImageJ.

Cardiovascular assessment

Ventricular and aortic function were evaluated using the Vevo 770 echocardiography system (Visualsonic, Toronto, Canada). In brief, mice were anesthetized with isofluorane and cardiac and aortic images were acquired using 15-45 MHz (RMV707B) and 20-60 MHz (RMV704) transducers, respectively. Transthoracic M-mode images of the heart were obtained in parasternal short axis at the level of the papillary muscle to determine left ventricular dimensions, fractional shortening, and cardiac output. Additionally, B-mode images of the thoracic aorta were obtained in a longitudinal plane to measure end-systolic and end-diastolic diameters of the distal ascending aorta. In a subgroup of animals, cardiovascular function was also invasively evaluated using a high-fidelity 1.9 French transducer-tipped catheter (Millar Inc., Houston, TX). In brief, mice were anesthetized by ketamine injection, supported on a ventilator, and maintained on isofluorane inhalation. The transducer-tipped catheter was advanced into the left ventricle via the right carotid artery. Pressures and volumes were recorded under basal conditions and with gradually increasing doses of dobutamine infusion from 0-4 μg/kg/min. Data were recorded by MacLab software and then analyzed by the Heartbeat program.

Serological analyses

Blood was collected in Eppendorf tubes and serum was obtained after clot removal. Alternatively, blood from EDTA-coated tubes was separated into cellular and plasma components by centrifugation. Lipid levels were measured using Amplex Red Cholesterol Assay Kits (Invitrogen, Grand Island, NY) and Triglyceride Determination Kits (Sigma-Aldrich), respectively. IgG and IgM plasma levels were quantified using ELISA kits (Bethyl Laboratories, Montgomery, TX). Plasma cytokines were evaluated using a Luminex-based multicytokine kit (Millipore, Billerica, MA) according to the manufacturer's protocol. In brief, specimens and standards were sequentially incubated with premixed antibody-coated bead sets, detection antibodies, and streptavidin-phycoerythrin. Reporter fluorescence of the beads was determined using a Luminex 200 analyzer, samples were run in duplicate and quantified based on a unique standard curve for each analyte. IFN-γ plasma levels were also determined in additional samples using a sandwich ELISA kit (Millipore) following the manufacturer's instructions.

Flow cytometry

Blood was collected in EDTA-coated tubes, cells were separated by centrifugation, and red blood cells were lysed with ACK buffer. Splenocytes were obtained after mincing and straining tissue, centrifugation, and red blood cell lysis. For isolation of artery-infiltrating leukocytes, aortas were digested with 125 U/mL collagenase XI, 60 U/mL hyaluronidase I, 60 U/mL DNase 1, and 450 U/mL collagenase I (Sigma-Aldrich) in phosphate-buffered saline containing 20 mM HEPES at 37 °C for 1-2 h. The tissue and supernatant were resuspended in RPMI-1640 medium at 4 °C and passed through 0.5 and 0.1 mm sieves. Leukocytes were isolated with CD45 antibody-coated magnetic beads (Miltenyi Biotec, Auburn, CA) and cell separation columns; selected cells were >95% $CD45^+$. Cell surface molecules were labeled with fluorescence-conjugated monoclonal antibodies to CD4, CD5, CD8, CD11b, CD25, CD43, CD45, CD69, B220, Ly6C, Ly6G (all from eBioscience, San Diego, CA), CCR2 (R&D, Minneapolis, MN), or isotype-matched, irrelevant IgG (eBioscience). For intracellular staining, the cells were treated with phorbol myristate acetate at 10 ng/mL and ionomycin at 1 μM for 5 h in the presence of brefeldin A at 10 μg/mL, labeled with antibodies to cell surface markers, fixed with 4% paraformaldehyde and permeabilized with 0.1% w/v saponin, and then labeled with PE-conjugated, rat anti-mouse IFN-γ, FITC-conjugated rat anti-mouse IL-17, or fluorescence-conjugated, isotype-matched, irrelevant antibodies (eBioscience). Additionally, cultured lung microvascular endothelial cells and aortic smooth muscle cells from C57BL/6 mice were incubated with serum (1:1,000 dilution) from various recipients and surface bound immunoglobulin was detected using rat anti-mouse IgG (Invitrogen). Analysis was performed using a LSR II system (BD Biosciences, San Jose CA) and FlowJo software (BD Biosciences).

Immunofluorescence microscopy

Five μm-thick sections of OCT-embedded heart specimens were fixed in acetone and sequentially labeled with rat anti-mouse CD31 monoclonal antibody (BD Biosciences) followed by Alexa Fluor 594-conjugated anti-rat IgG (Invitrogen), and then by Alexa Fluor 488-conjugated rat anti-mouse I-A/I-E monoclonal antibody (Biolegend, San Diego, CA). Alternatively, myocardium sections were labelled with antibodies to IgG (Invitrogen), CD31, and smooth muscle α-actin (Santa Cruz Biotechnology) and aortic root sections were labelled with antibodies to CD3, F4/80 (Abcam, Cambridge, MA), B220, and Ly6G (eBioscience). Controls included isotype-matched, irrelevant IgG. The specimens were mounted with ProLong Gold antifade reagent with DAPI (Invitrogen). Images were acquired using an Axiovert 200M microscopy system (Carl Zeiss MicroImaging, Thornwood, NY) with Volocity 6.3 software (PerkinElmer, Waltham, MA).

Real-time quantitative RT-PCR

Serial sections of OCT-embedded tissue were immersed in RLT lysis buffer (QIAGEN, Valencia, CA), vigorously vortexed, and total RNA was isolated using Rneasy mini kits and DNA digestion kits (QIAGEN) according to the manufacturer's protocol. RT with random hexamer and oligo-dT primers was performed according to the Multiscribe RT system protocol (Applied Biosystems, Foster City, CA). RT-PCR reactions were prepared with TaqMan PCR Master Mix and predeveloped assay reagents from Applied Biosystems. Duplicate samples were analyzed on an iCycler (Bio-Rad Laboratories, Hercules, CA). RNA samples processed without the RT enzyme were used as negative controls. The expression of IFN-γ, CXCL10, IL12a, and IL-18 transcripts were normalized to GAPDH; a second reference gene of β-actin gave similar results.

Supplemental Figures and Figure Legends

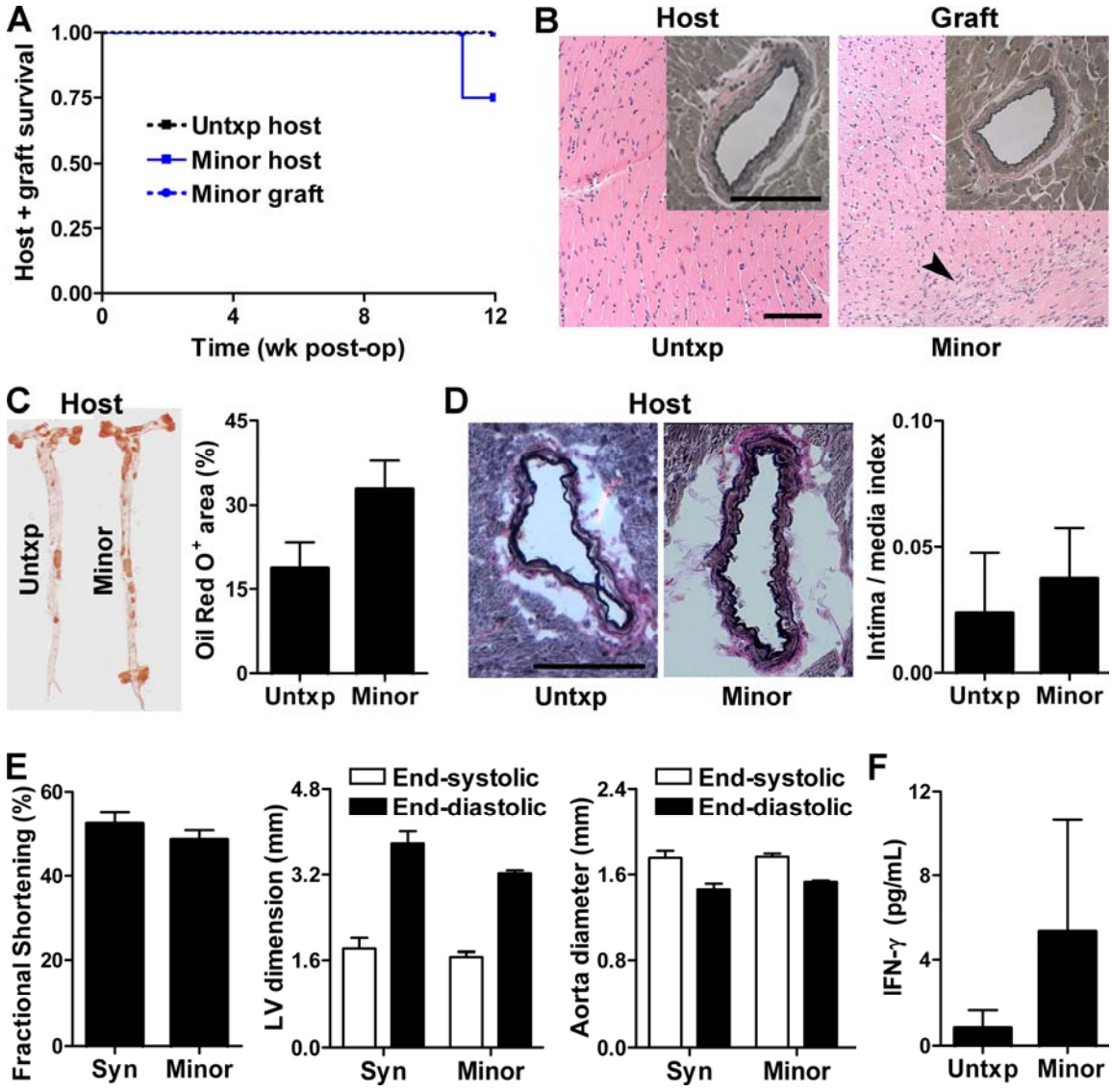

Online Figure I. Single minor histocompatibility antigen mismatch. (*A*) Survival of 30 wk old C57BL/6 ApoE$^{-/-}$ female mice either untransplanted (Untxp) or receiving syngeneic male heterotopic cardiac grafts, all grafts were beating at 12 wk post-op; *n*=4, *P*=0.37. (*B*) Representative photomicrographs of the native heart or of the donor graft in a minor-mismatched recipient at 12 wk post-op showing mild cellular infiltrates (arrowhead, H&E stain) and minimal neointima (inset, EVG stain), bars=100 μm. (*C*) Representative Oil Red O stains of the host aorta and expressed as % total area; *n*=3-4, *P*=1.0 vs. Untxp. (*D*) Representative EVG stains of host coronary artery frozen sections showing minimal neointima, bar=100 μm and expressed as intima to media area index; *n*=13-17 coronary arteries of >50 μm diameter from 3-4 recipients, *P*=0.67 vs. Untxp. (*E*) Left ventricular fractional shortening, left ventricular internal dimensions, and ascending aorta diameters at end-systole and end-diastole of female recipients of male grafts and male recipients of male grafts; *n*=3-4, *P*>0.05 vs. Syn. (*F*) Plasma levels of IFN-γ in untransplanted and minor-mismatched recipients; *n*=3-4, *P*>0.05 vs. Untxp.

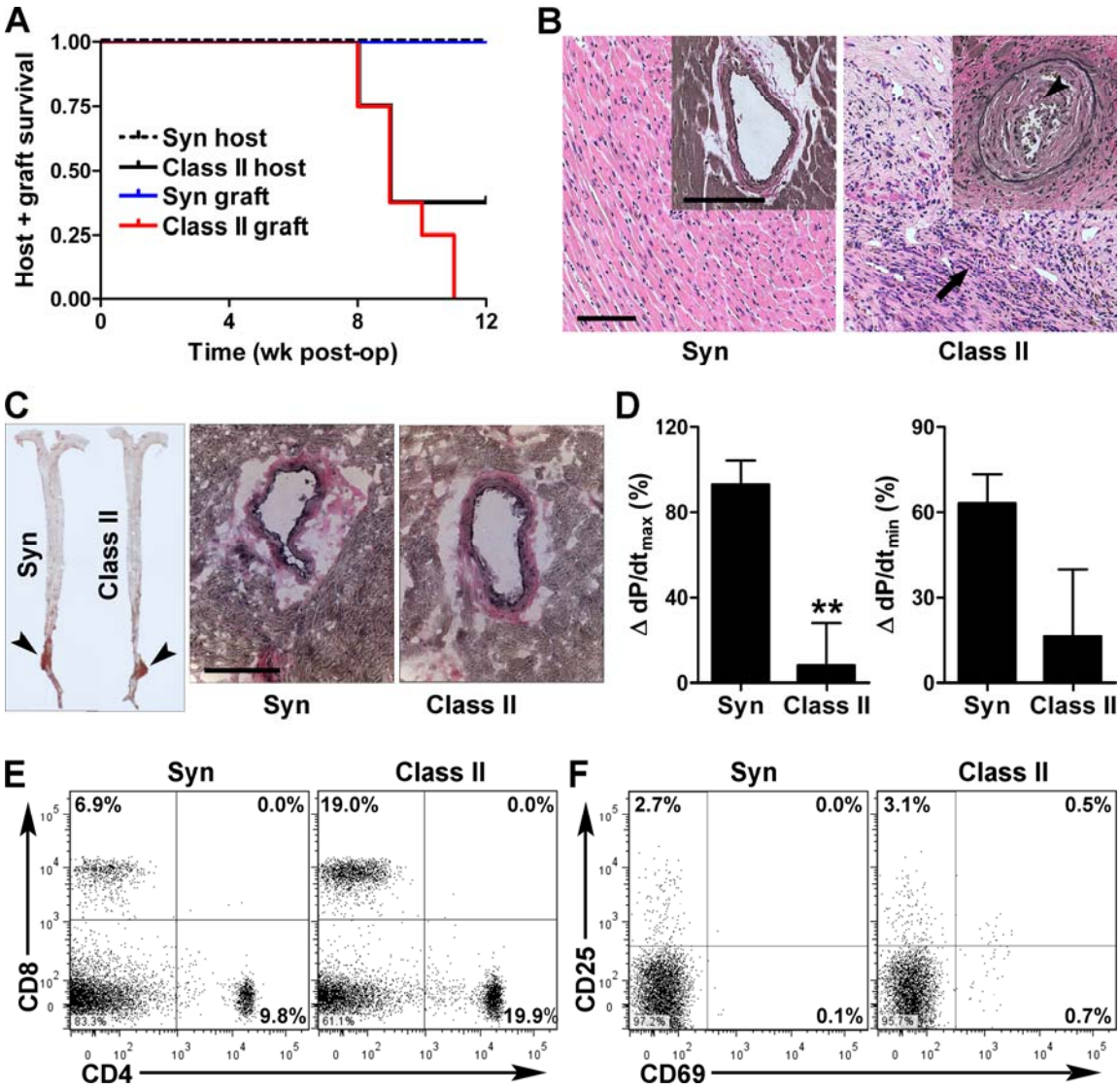

Online Figure II. Normolipidemic recipients of class II-mismatched cardiac grafts. (*A*) Survival of 30 wk old C57BL/6 male mice after transplantation with syngeneic or bm12 male heterotopic cardiac grafts; n=8, P<0.001. (*B*) Representative photomicrographs of the donor grafts at 12 wk post-op showing cardiomyocyte destruction with cellular infiltrates (arrow, H&E stain) and coronary artery neointima formation (inset, arrowhead, EVG stain), bars=100 μm. (*C*) Representative Oil Red O stains of the host aorta and EVG stains of host coronary artery frozen sections at 12 wk post-op showing no lipid accumulation (besides nonspecific uptake at anastomotic sites, arrowheads) and no neointima, bar=100 μm. (*D*) Change in dP/dt_{max} and dP/dt_{min} from basal to stress conditions after dobutamine infusion at 4 μg/kg/min; n=4-8, **P<0.01 vs. Syn. (*E*) CD4 and CD8 expression by circulating mononuclear leukocytes at 12 wk post-op. (*F*) Circulating $CD4^+$ T cells were further analyzed for CD25 and CD69 expression.

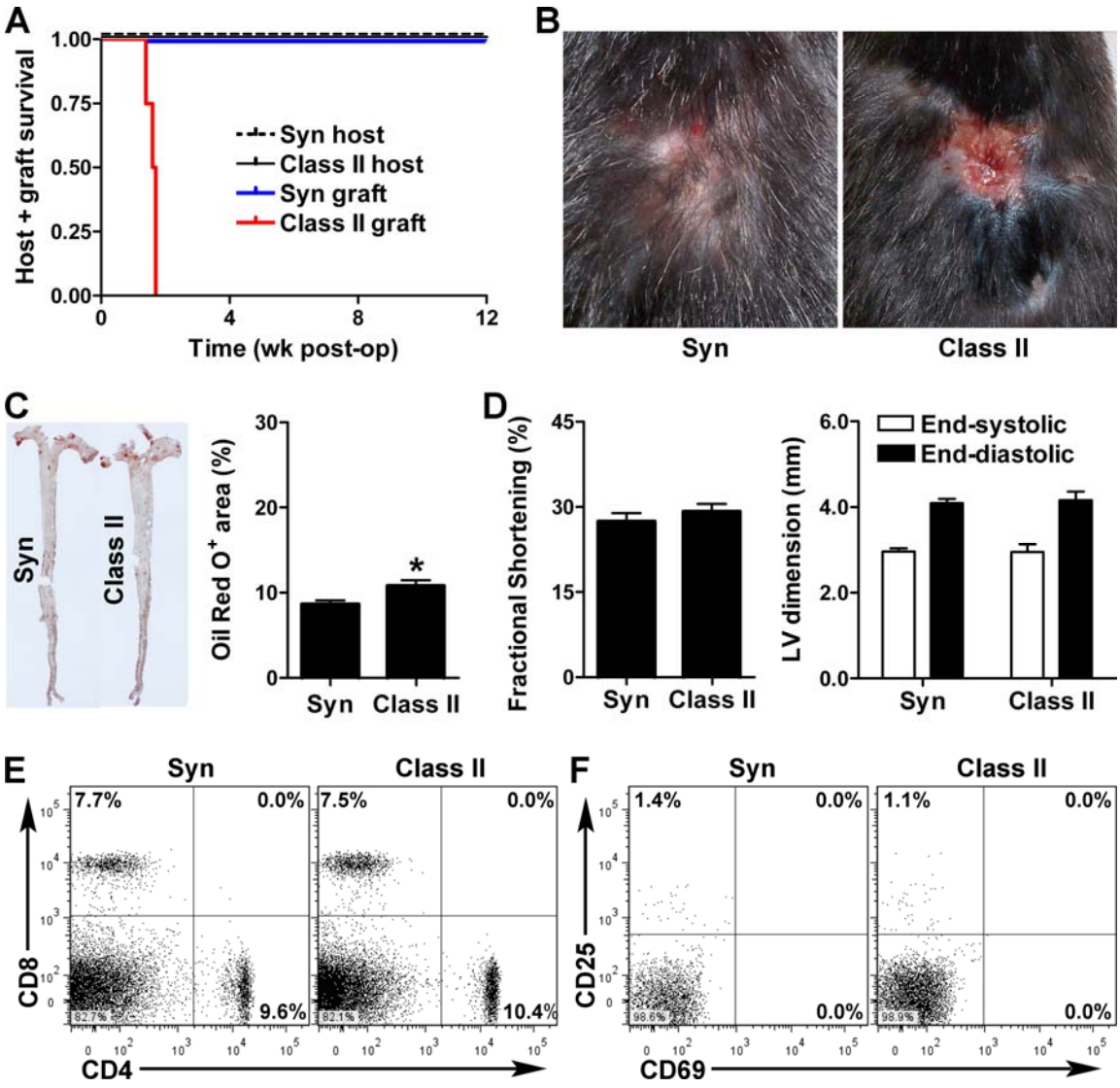

Online Figure III. MHC class II antigen disparate skin grafts to ApoE$^{-/-}$ recipients. (*A*) Survival of 30 wk old C57BL/6 ApoE$^{-/-}$ male mice after grafting with syngeneic or bm12 male skin; *n*=4, *P*<0.001. (*B*) Representative photographs of the grafts at 3 wk post-op showing rejection of allogeneic not syngeneic skin. (*C*) Representative Oil Red O stains of the host aorta and expressed as % of total area; *n*=4, **P*<0.05 vs. Syn. (*D*) Left ventricular fractional shortening and left ventricular internal dimensions at end-systole and end-diastole at 12 wk post-op; *n*=4, *P*>0.05 vs. Syn. (*E*) CD4 and CD8 expression by circulating mononuclear leukocytes at 12 wk post-op. (*F*) Circulating CD4^{+} T cells were further analyzed for CD25 and CD69 expression.

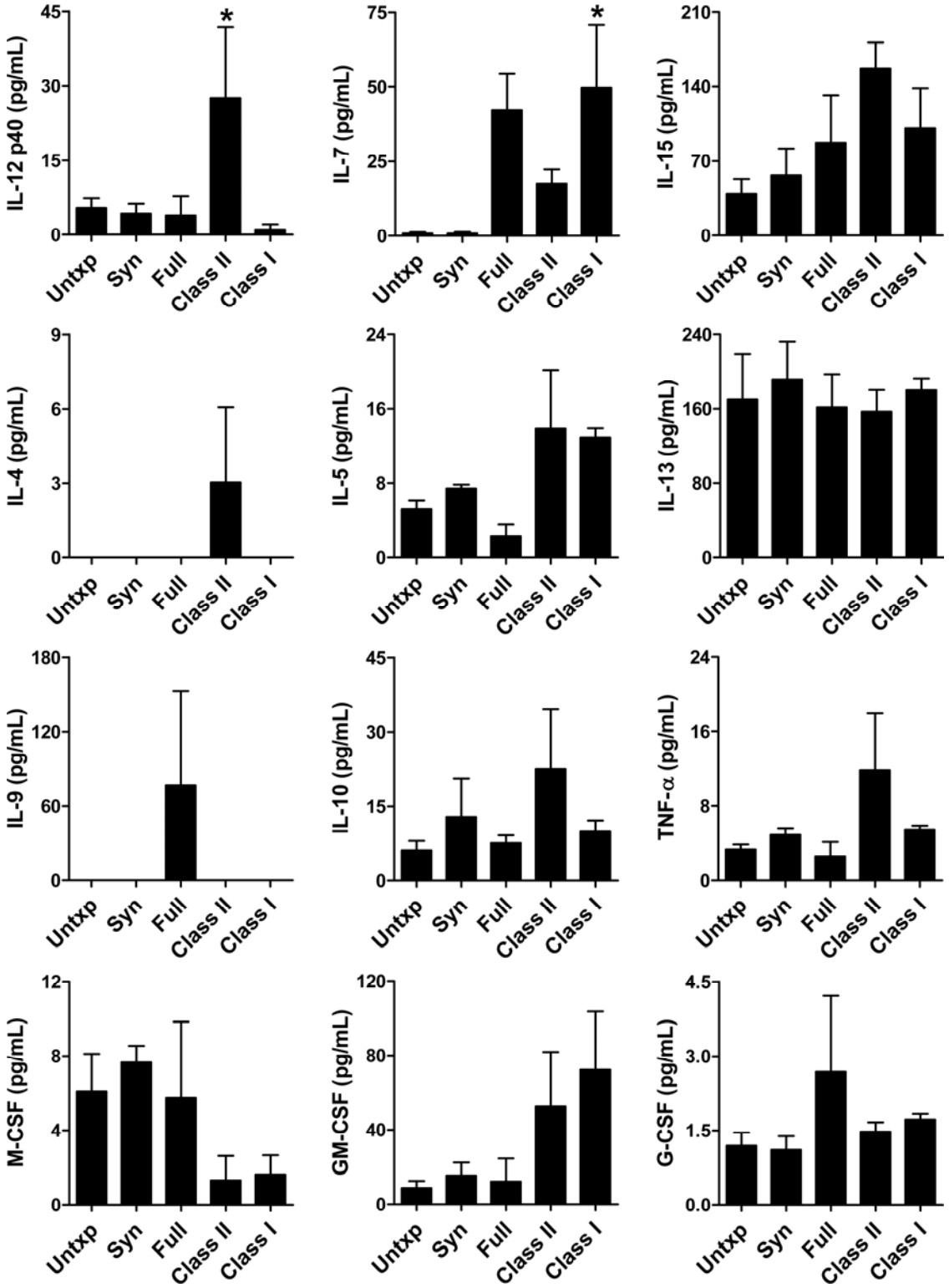

Online Figure IV. Circulating levels of lymphocyte- and macrophage-derived cytokines. Plasma levels of IL-12 p40, IL-7, IL-15, IL-4, IL-5, IL-13, IL-9, IL-10, TNF-α, M-CSF, GM-CSF and G-CSF were measured by multiplex bead-based immunoassay in untransplanted ApoE$^{-/-}$ mice or in ApoE$^{-/-}$ recipients of syngeneic or full-, class II- and class I-mismatched grafts at 12 wk post-op; *n*=3-8, **P*<0.05 vs. Untxp and Syn.

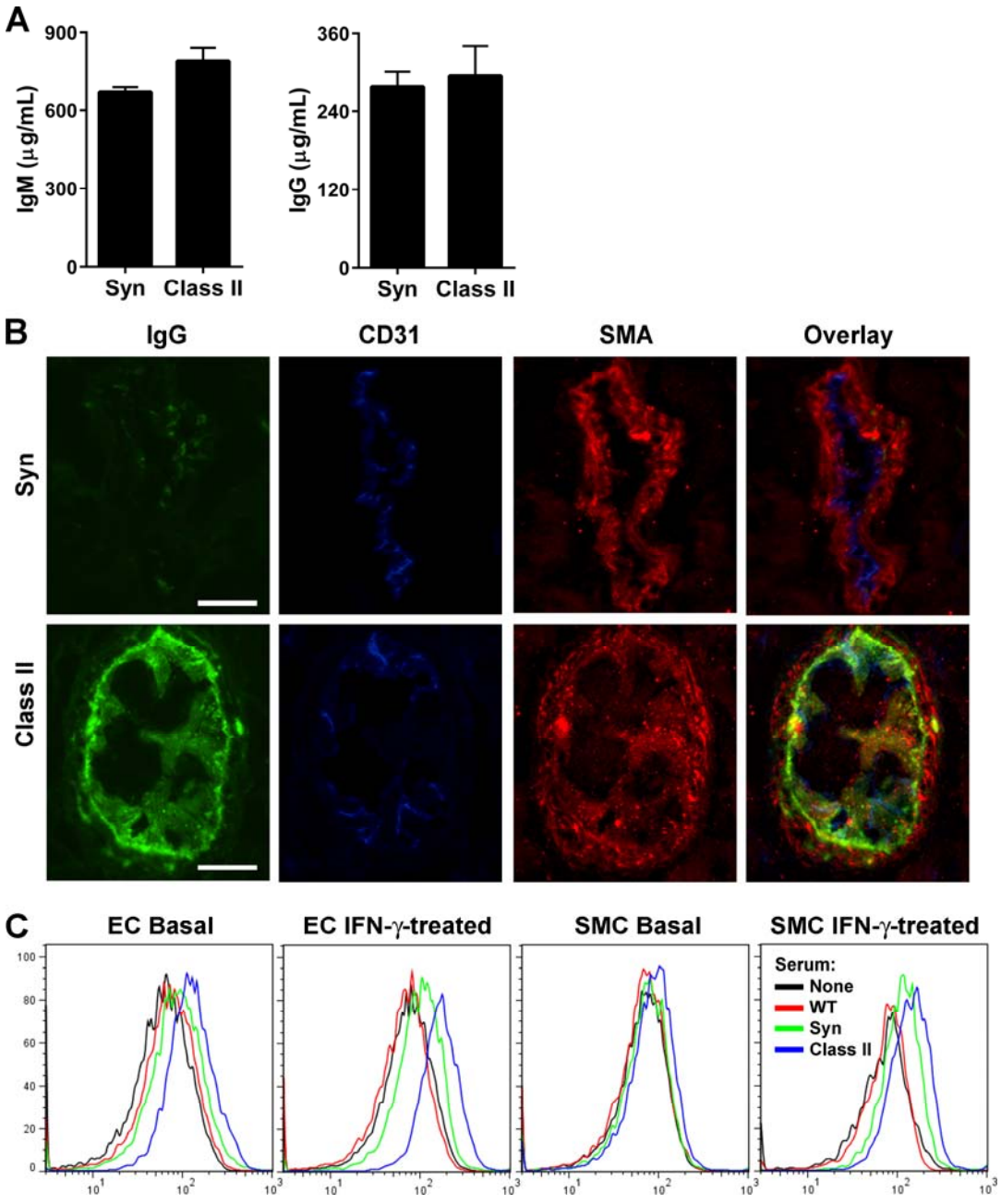

Online Figure V. Antibody deposition in host coronary arteries. (*A*) Plasma levels of IgM and IgG in ApoE$^{-/-}$ recipients of syngeneic and class II-mismatched grafts at 12 wk post-op; *n*=4, **P*=0.062 and 0.75, respectively. (*B*) Representative images of immunofluorescence analysis of native coronary arteries from ApoE$^{-/-}$ recipients of syngeneic (upper panels) and class II-mismatched (lower panels) grafts for IgG (green color), CD31 (blue color), smooth muscle α-actin (red color), and overlay of images to demonstrate immunoglobulin deposition on host endothelium and neointimal (but not medial) smooth muscle cells in vivo, bars=50 μm. (*C*) Flow cytometric analysis to detect reactivity of IgG in serum (1:1,000 dilution) from wild-type C57BL/6 mice or ApoE$^{-/-}$ recipients of syngeneic and class II-mismatched grafts to autologous cultured endothelial cells and smooth muscle cells either untreated or treated with IFN-γ (10 ng/mL x 3 d) in vitro. Cytokine treatment increased the expression of cell surface molecules binding autoreactive serum antibodies present in ApoE$^{-/-}$ transplant recipients, particularly of class II-mismatched grafts.

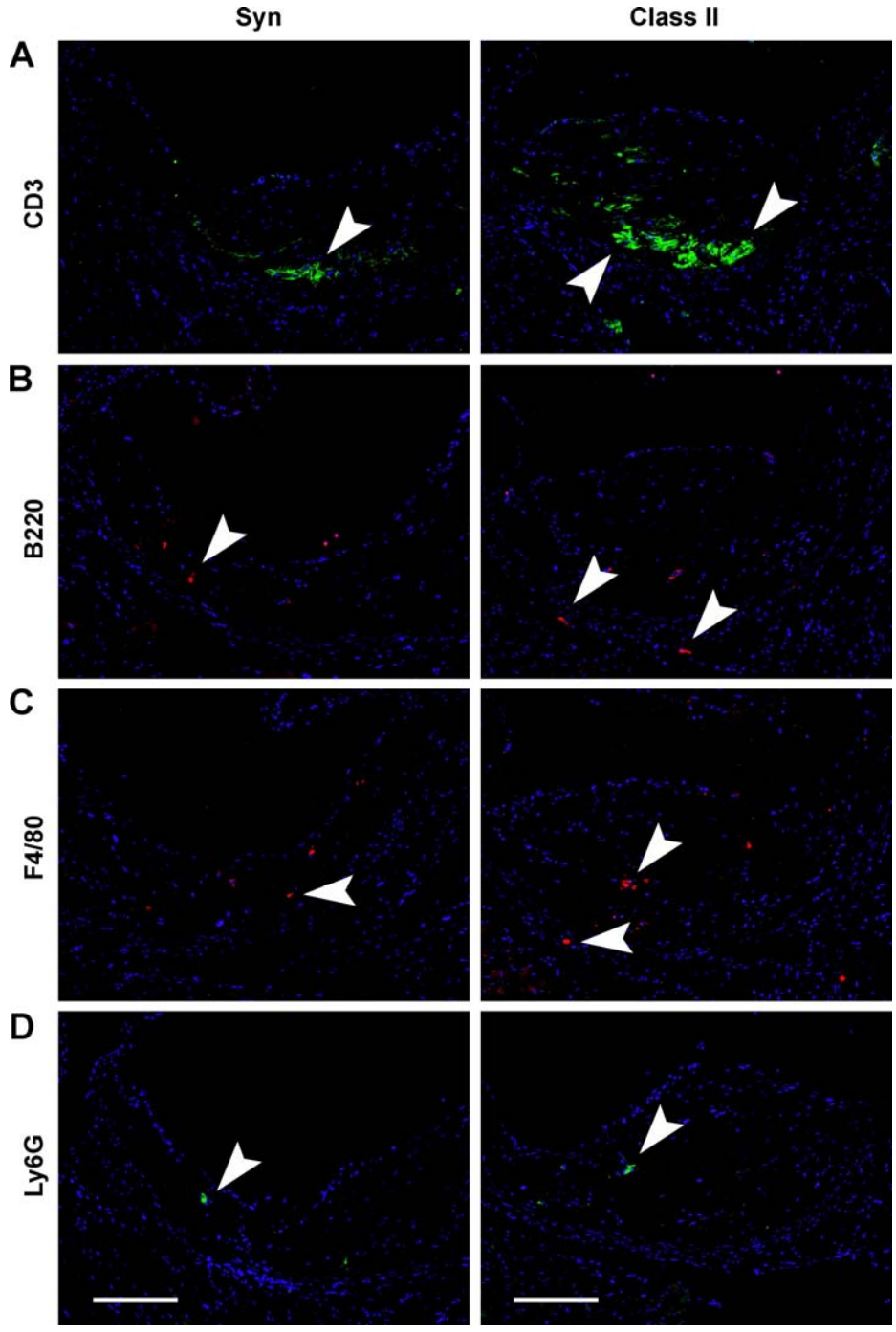

Online Figure VI. Leukocytic infiltrates in atherosclerotic lesions of the host aorta. Representative images of immunofluorescence analysis of native aortic roots from ApoE$^{-/-}$ recipients of syngeneic (left panels) and class II-mismatched (right panels) grafts for (*A*) CD3 T cell marker (green color), (*B*) B220 B cell marker (red color), (*C*) F4/80 macrophage marker (red color), and (*D*) Ly6G granulocyte marker (green color) overlayed with DAPI nuclear staining (blue color) to differentiate aortic annular tissue (below) from lumen (above), bars=200 μm. The atherosclerotic lesions of allografted recipients demonstrated a greater infiltrate of mononuclear leukocytes, particularly of T cells, but a similar sparse granulocyte infiltrate to syngeneic grafted recipients.

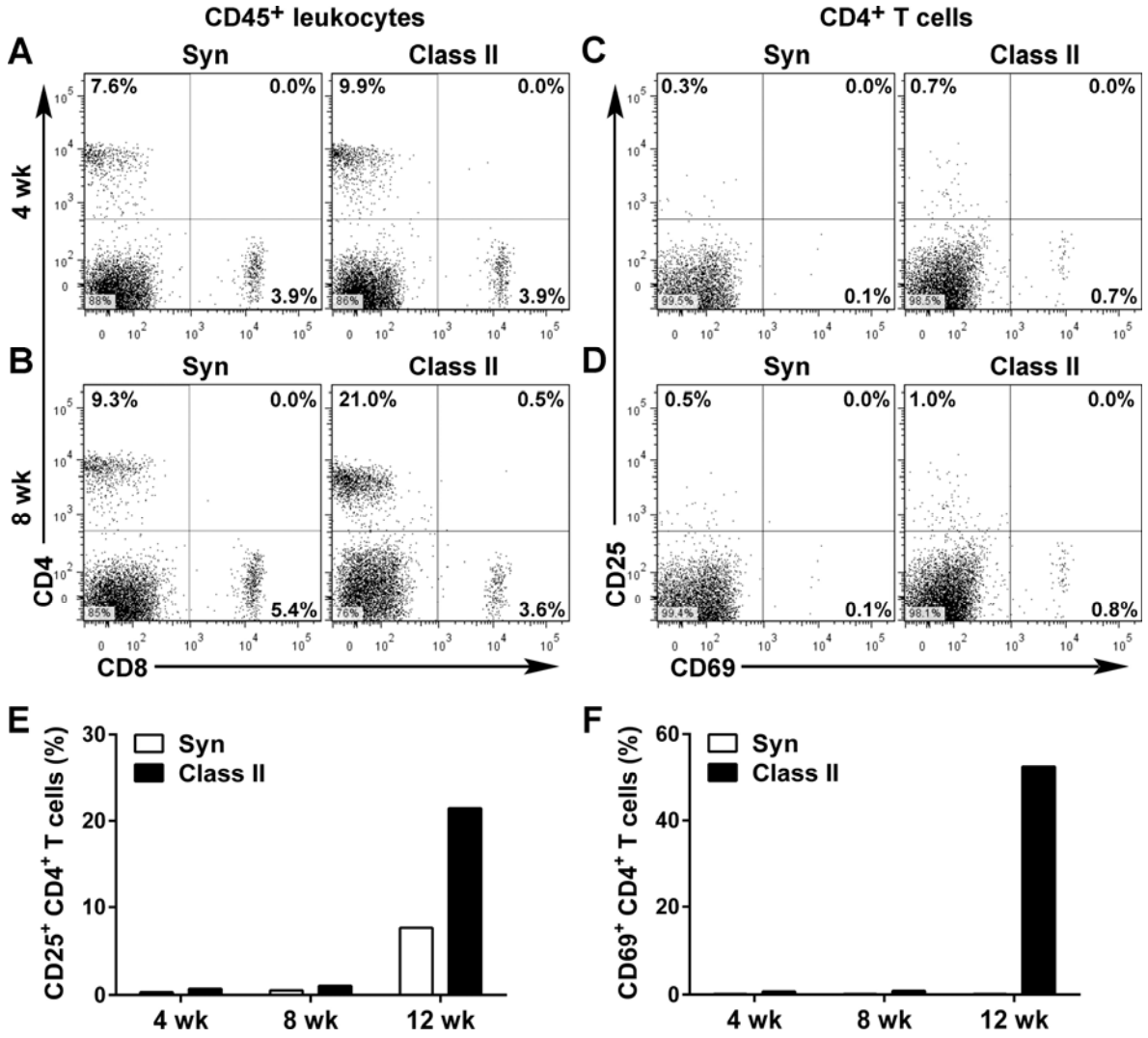

Online Figure VII. T cell phenotype at different times after transplantation. Flow cytometric analysis was performed on circulating mononuclear leukocytes pooled from 3 ApoE$^{-/-}$ recipients of syngeneic or class II-mismatched grafts. CD4 and CD8 expression by CD45^{+} leukocytes at (*A*) 4 wk and (*B*) 8 wk post-op (corresponding dot-plots at 12 wk post-op are shown in Fig. 5). Further analysis of the CD4^{+} T cell population for CD25 and CD69 expression at (*C*) 4 wk and (*D*) 8 wk post-op (corresponding dot-plots at 12 wk post-op are also shown in Fig. 5). Temporal trend of (*E*) CD25 expression by circulating CD4^{+} T cells and (*F*) CD69 expression by circulating CD4^{+} T cells.

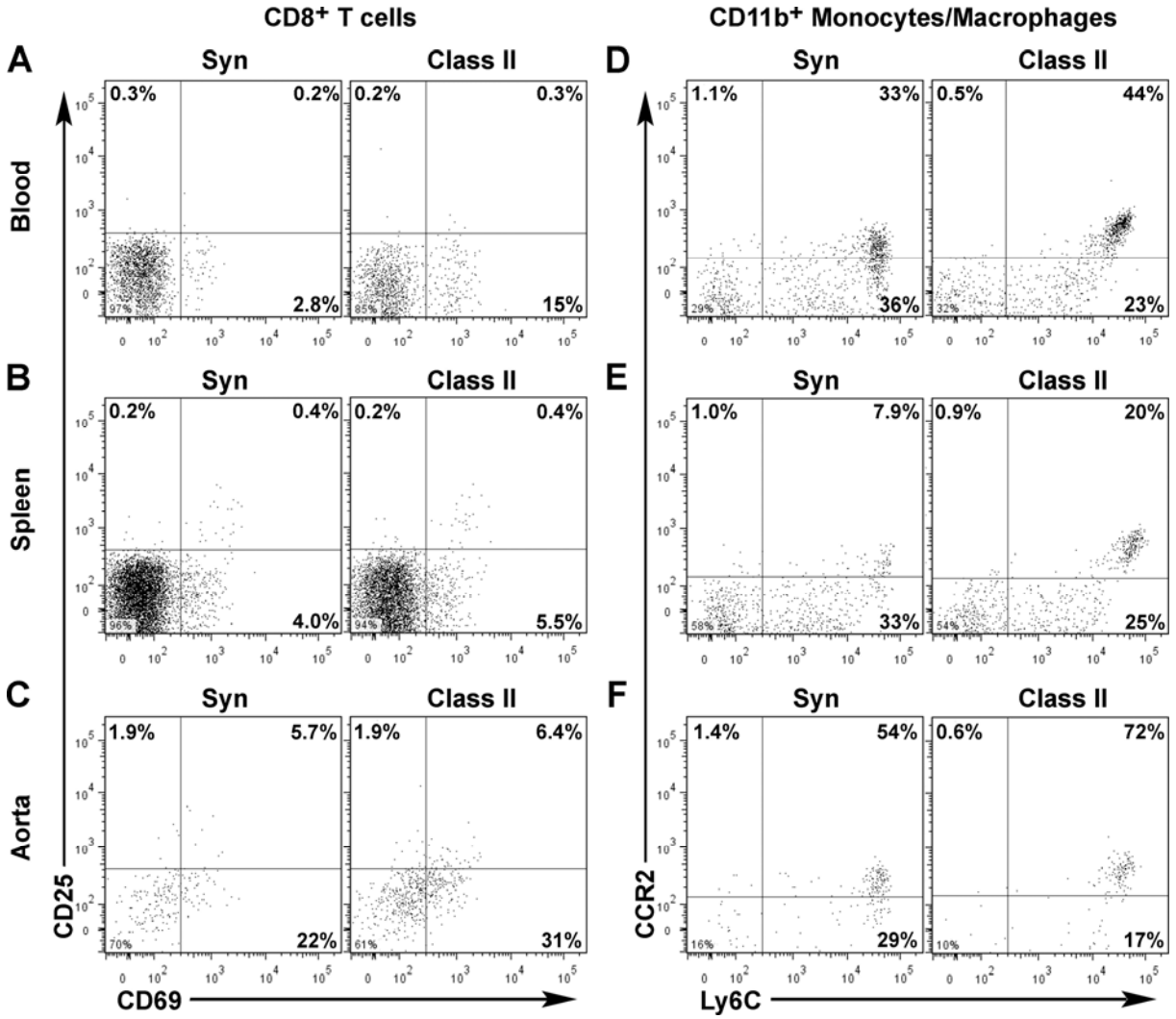

Online Figure VIII. Phenotype of cytotoxic T cells and monocyte/macrophages. Leukocyte phenotypes were characterized by flow cytometry in ApoE$^{-/-}$ recipients of syngeneic and class II-mismatched grafts at 12 wk post-op. Expression of the activation markers, CD25 and CD69 by CD8^{+} T cells isolated from (*A*) blood, (*B*) spleen, and (*C*) host aorta. CD11b^{+} monocyte/macrophages from (*D*) blood, (*E*) spleen, and (*F*) host aorta were also analyzed for the expression of the inflammatory markers, CCR2 and Ly6C to define subsets of CCR2^{-}/Ly6C^{low} patrolling monocytes and CCR2^{+}/Ly6C^{high} inflammatory monocytes.

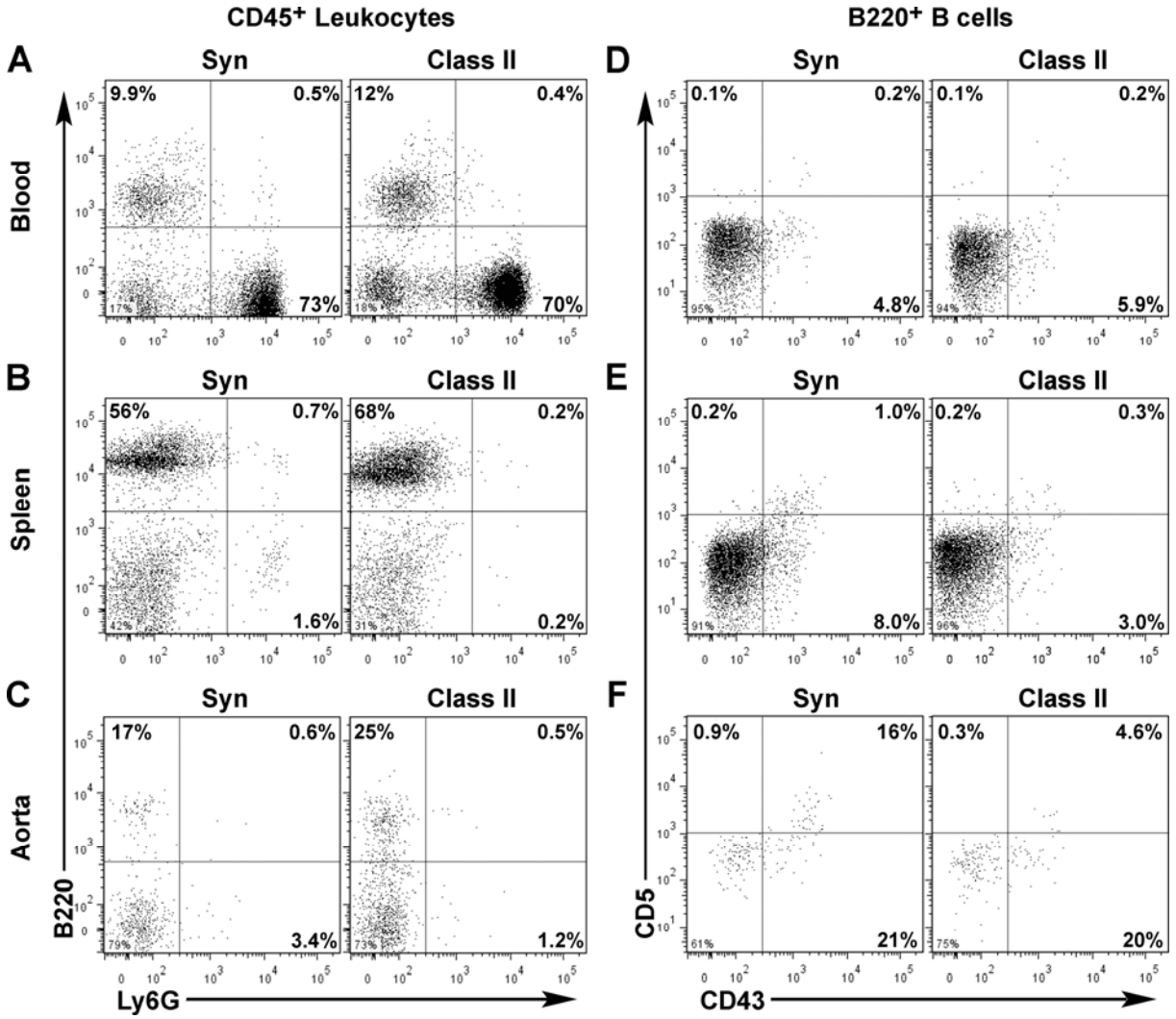

Online Figure IX. Phenotype of B cells and neutrophils. Leukocyte phenotypes were characterized by flow cytometry in ApoE$^{-/-}$ recipients of syngeneic and class II-mismatched grafts at 12 wk post-op. Expression of the B cell marker, B220 (CD45R isoform) and the neutrophil marker, Ly6G by CD45^{+} leukocytes isolated from (*A*) blood, (*B*) spleen, and (*C*) host aorta. B220^{+} B cells from (*D*) blood, (*E*) spleen, and (*F*) host aorta were further analyzed for the expression of CD5 and CD43 to define subsets of CD5^{+}/CD43^{+} B-1a cells, CD5^{-}/CD43^{+} B-1b cells, and CD43^{-}/CD5^{-} B-2 cells.

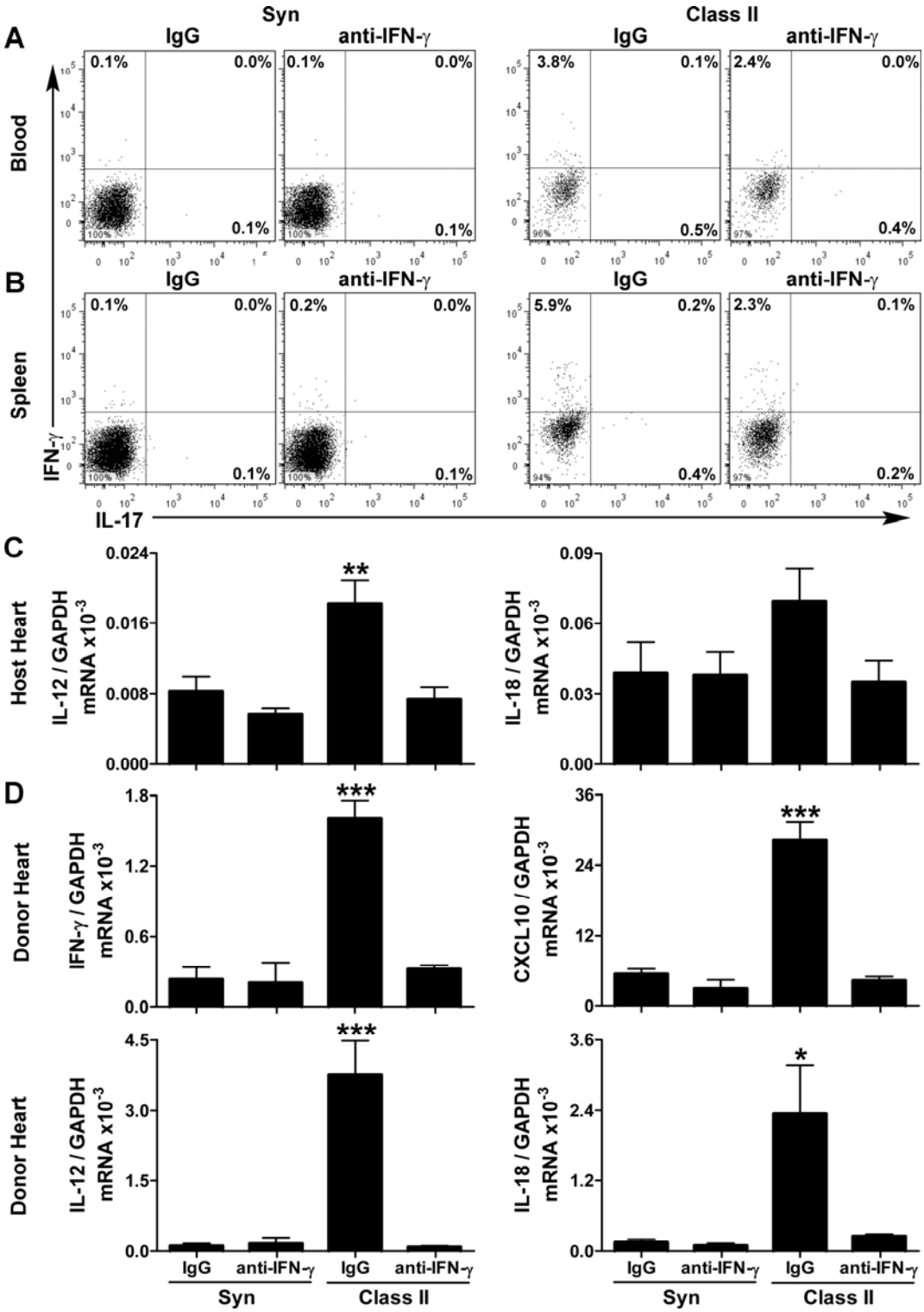

Online Figure X. Effects of IFN-γ neutralization on immune and inflammatory responses. (*A*) IFN-γ and IL-17 expression by circulating CD45^{+} leukocytes not expressing CD4 in ApoE$^{-/-}$ recipients of syngeneic and class II-mismatched grafts treated with irrelevant IgG or anti-IFN-γ antibody (cells pooled from 3 animals). (*B*) Similar analyses in splenic cells. (*C*) Quantitative RT-PCR of recipient hearts for IL-12 and IL-18 RNA. (*D*) Similar analysis of donor grafts for IFN-γ, CXCL10, IL-12, and IL-18 transcripts. *n*=3-5, **P*<0.05, ***P*<0.01, ****P*<0.001, vs. other groups.

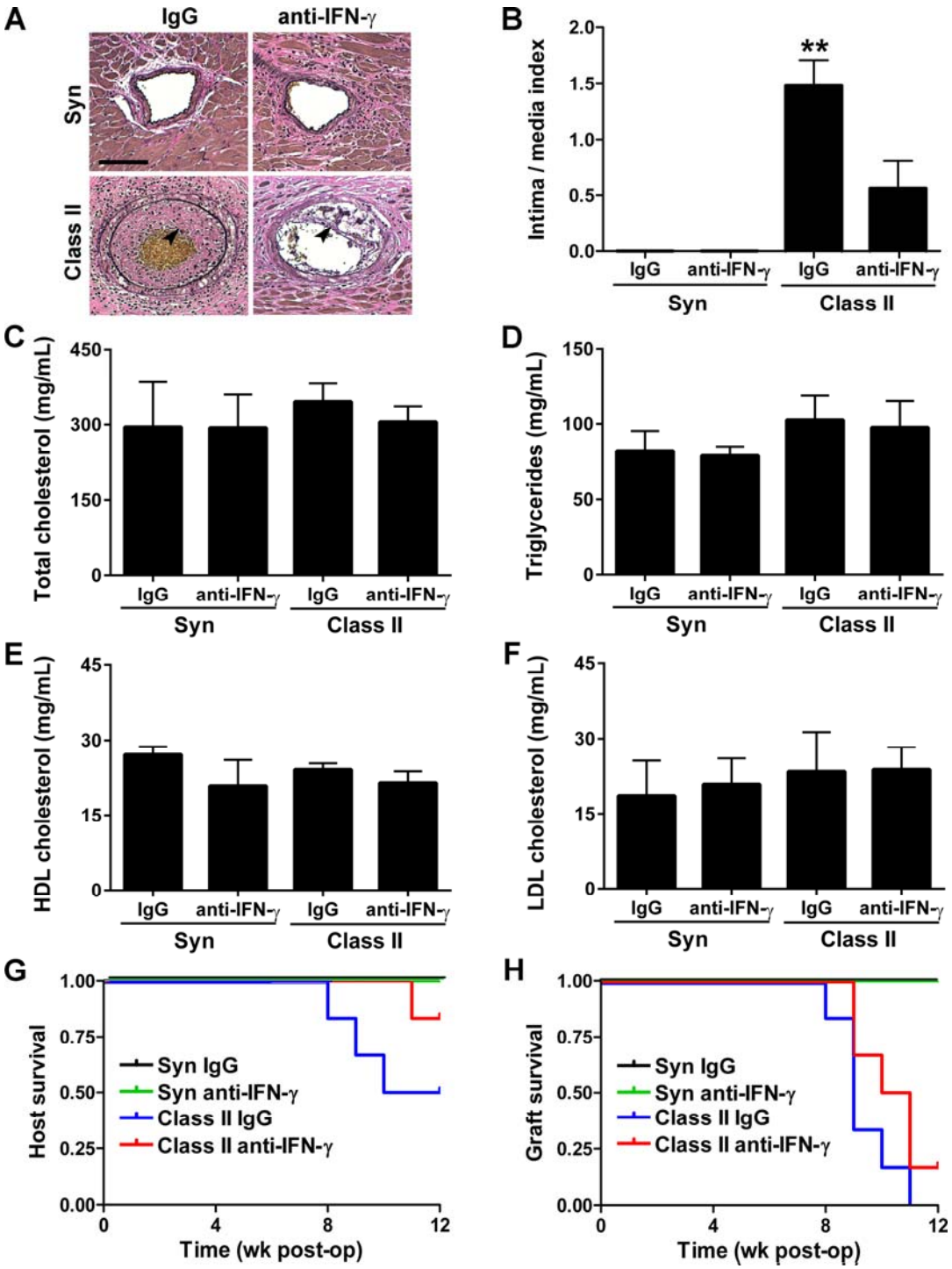

Online Figure XI. Effects of IFN-γ neutralization on graft and host CVD. ApoE$^{-/-}$ recipients of syngeneic or class II-mismatched grafts were treated with irrelevant IgG or anti-IFN-γ antibody from 0-12 wk post-op. (*A*) Representative EVG stains of donor heart graft frozen sections at 12 wk post-op showing coronary artery neointima (arrowheads, bar=100 μm) and (*B*) expressed as a ratio of intima to media area; n=3-5, $^{**}P$<0.01 vs. other groups. (*C*) Total cholesterol, (*D*) triglyceride, (*E*) HDL cholesterol, and (*F*) LDL cholesterol plasma levels of hosts at 8-12 wk post-op; n=3-5, P>0.05. (*G*) Host survival; n=3-6, P=0.18 for Class II IgG vs. Class II anti-IFN-γ and (*H*) graft survival; n=3-6, P=0.10 for Class II IgG vs. Class II anti-IFN-γ.